

Journal of Mathematical Extension  
Vol. XX, No. XX, (2014), pp-pp (Will be inserted by layout editor)  
ISSN: 1735-8299  
URL: <http://www.ijmex.com>

## Image Zooming Using Barycentric Rational Interpolation

**Ali Mohammad Esmaili Zaini**

PhD candidate in Applied Mathematics, Department of Applied Mathematics, Yazd University, Yazd, Iran.

**Ghasem Barid Loghmani \***

Professor, Department of Applied Mathematics, Yazd University, Yazd, Iran.

**Ali Mohammad Latif**

Associate Professor, Department of Computer Engineering, Yazd University, Yazd, Iran.

**Abstract.** Image zooming is one of the important issues of image processing that maintains the quality and structure of image. Zooming an image necessitates placing the extra pixels in the image data. Moreover, adding the data to the image must be consistent with the texture in the image in order to prevent artificial blocks. In this study, the required pixels are estimated using barycentric rational interpolation. The proposed method is a non-linear one which can preserve the edges and reduces the blur and block artifacts on the zoomed image. Numerical results are presented using PSNR and SSIM fidelity measures and they are compared to some other methods. The average PSNR of the original image and image zooming was 33.08 which can prove that image zooming is very similar to the original image. The experimental results revealed that the proposed method had a better performance compared to other methods and could provide good image quality.

---

Received: XXXX; Accepted: XXXX (Will be inserted by editor)

\*Corresponding Author

**Keywords and Phrases:** : Image zooming, Barycentric rational formula, Rational function, Interpolation.

## 1 Introduction

The fundamental aim of image zooming is to increase the resolution of the image in order to achieve an appropriate image quality. It plays an important role in image processing and machine vision, and enjoys a variety of applications in printing industry, electronic publishing, digital cameras, medical imaging and sampling, images on web pages, license plate recognition, as well as face recognition systems [1].

Recent studies have revealed that in many of these applications, the main focal task regards the visual quality of images. Both resolution of the edges and lack of blurred and additional artifacts are the two important factors involved in enhancing the quality of zoomed images.

The interpolation method is used in most algorithms of image zooming. The aim is to find a set of unknown pixel values from a set of known pixel values in the image.

In image zooming, several basic parameters affect image quality, including:

1. Zooming should preserve the edges and borders of the image.
  2. The magnification method should not produce undesirable piecewise constant or artificial blocks.
  3. Zooming method should not have high computational complexity [2].
- Traditional technologies used linear interpolation methods in order to create high resolution samples in zooming images. Pixel replication, bi-linear interpolation, quadratic interpolation, bi-cubic interpolation, and spline interpolation can be counted as some of the linear interpolation methods [3-6]. These methods serve not only to smooth out image edges, but, in some cases, also to produce stair edges. Moreover, the outputs of these methods are blurred images.

In recent years, modification of the linear methods in terms of improving image quality and solving the problem of image blur has been done using non-linear interpolation technique. These methods perform differently with sharp and soft edges. In fact, these methods are in contrast with the linear methods that treat similar to all pixels [7-9].

In such non-linear methods, after estimation of a subset of edge pixels [8], resampling, parameter optimization, contextual interpolation, and edge direct interpolation are conducted to enhance the image quality and edges [10-13].

In [10], statistical methods were used to set the structure of the edges, and correction technique of bi-linear interpolation, and interpolation error theorem [11] were used in an edge-adaptive method.

In [14], as a part of the edge-directed non-linear interpolation method, the technique of filtering direction and data fusion was employed, and a missed pixel was interpolated in different directions. Then, the results of edge-directed interpolation were combined with linear least squares estimations, and therefore the desired outcome could be reached.

In [15], LAZ method was introduced as a local adaptive zooming algorithm with the purpose of finding the edges in different directions through using the information from discontinuity or sharp brightness variations. Two threshold values were also considered, and the missing pixels were estimated regarding the direction of the edge.

More recently, some new methods based on partial differential equations (PDEs) have also been proposed and could have shown better performances than the previous methods. In [16-17], edge-directed interpolation methods were discussed founded on diverse issues regarding PDEs. [18] presented non-linear curvature interpolation method and PDEs for image-zooming were. In another study [19], non-linear fourth-order PDEs method was a new combination of the locally adaptive zooming algorithm for image zooming. An image zooming algorithm was offered using non-linear PDE, combined with edge-directed bi-cubic algorithm in [20].

It is notable that most PDE-based methods can provide clear images with sharp edges. The negative effects resulting from blurring and artificial blocks have been reduced to a minimum in these methods.

In another study [21], a non-linear image-zooming method was proposed based on radial basis functions and contextual edge correction techniques. Given that the radial basis functions have the shape parameter  $c$ , this method introduces an interval for  $c$  by conducting numerical experiments.

Similar studies offer other methods for zooming purposes, for example,

in [22], artificial neural network methods have been used for zooming operations on digital images; in [23], a non-linear image interpolation algorithm based on moving least squares technique has been presented and the ability for image zooming and preserving edge features is demonstrated.

In [24], image zooming by least squares surfaces has been presented in a way that extra pixels can be estimated using the surface of least squares. In [25], the required pixels have been estimated for image zooming through using the radial basis functions and calculating the shape parameter  $c$  with genetic algorithm.

Taking this literature into account, the present study, aims at estimating the required pixels in three steps in linear processes using barycentric rational interpolation.

The structure of this paper is as what follows. In Section 2, barycentric rational interpolation will be discussed. In Section 3, a discussion of image zooming will be provided. Section 4 focuses on presentation of the proposed method. The evaluation criteria and the results of the analyses and comparisons with other methods will be discussed in Section 5. In the final part, includes the concluding remarks and ideas for future research in this field.

## 2 Barycentric rational interpolation

In this section, we present a brief overview of the interpolation methods and Lagrange interpolation. Then, barycentric interpolation and barycentric rational interpolation will be described.

This study assumes that the values of the function at  $n$  distinct points  $(x_0, x_1, x_2, \dots, x_n) \in R$  are respectively equivalent to  $f(x_0), f(x_1), f(x_2), \dots, f(x_n)$ . Estimating the value of  $f(x), x_0 < x < x_n, x \neq x_i, i = 0, 1, \dots, n$  is defined as interpolation. The classical problem in this family is that of finding a unique polynomial  $P \in \prod_n$  of degree at most  $n$  such that  $P(x_i) = f(x_i), i = 1, 2, \dots, n$  [26].

In numerical analysis, for a given set of distinct points  $x_i$  and  $f_i, i = 0, 1, \dots, n$ , Lagrange polynomials are used for polynomial interpolation

[27]. The interpolation formula of Lagrange can be written as (1):

$$P(x) = \sum_{j=0}^n l_j(x) f_j, \quad l_j(x) = \prod_{k=0, k \neq j}^n \frac{x - x_k}{x_j - x_k} \quad (1)$$

In addition, the Lagrange polynomial  $l_j(x)$  corresponding to the node  $x_j$  has the property as (2):

$$l_j(x_i) = \begin{cases} 1 & j = i \\ 0 & j \neq i \end{cases} \quad (2)$$

But, as can be seen from the construction, each time a node  $x_j$  varies, all Lagrange basis polynomials have to be recalculated. However, a better form of the Lagrange interpolation can be rewritten (1). It is defined as:

$$l(x) = (x - x_0)(x - x_1) \dots (x - x_n) \quad (3)$$

$$w_j = \prod_{k=0, k \neq j}^n \frac{1}{x_j - x_k}, \quad j = 0, 1, \dots, n \quad (4)$$

Thus, we can write  $l_j(x)$  as

$$l_j(x) = \frac{l(x)w_j}{x - x_j} = \frac{l(x)}{l'(x_j)(x - x_j)} \quad (5)$$

It is clear that  $w_j = \frac{1}{l'(x_j)}$ . Therefore, the modified Lagrange formula can be written as (6), which does not depend on the point where the nodes are arranged.

$$P(x) = l(x) \sum_{j=0}^n \frac{w_j}{x - x_j} f_j \quad (6)$$

Since polynomial interpolation is unique, the constant function 1 is obviously interpolated by  $P(x) \equiv 1$ . Inserting the values into (6), we get:

$$1 = \sum_{j=0}^n l_j(x) = l(x) \sum_{j=0}^n \frac{w_j}{x - x_j} \quad (7)$$

Dividing equation (6) by this expiration and eliminating the common factor  $l(x)$ , we obtain the barycentric interpolation formula [28] for  $P$  as (8) where real values  $w_j$  are defined by (4).

$$P(x) = \frac{\sum_{j=0}^n \frac{w_j}{x-x_j} f_j}{\sum_{j=0}^n \frac{w_j}{x-x_j}} \quad (8)$$

As can be witnessed here, the barycentric formula is a Lagrange formula, but one with a special and beautiful symmetry. The weights  $w_j$  appear in the denominator exactly as in the numerator, except without the data  $f_j$ . Various aspects of this kind of interpolation have been survived in [29]. Thus, the weights in (4) prevent poles, but for interpolation points in a general position, they do not yield a good approximation. On the other hand, if  $x$  is equal to  $x_j$ , formula (8) cannot be used, because that would be a division of  $\infty$  by  $\infty$ . For cases of nonzero weights that differ from (4), formula (8) will still interpolate the data, but in general it will be a rational function which is not a polynomial. These rational barycentric interpolants can be very useful in some applications [30]. In [31] another option is discussed simply by taking  $w_j = (-1)^j, j = 0, 1, \dots, n$ . Then:

$$P(x) = \frac{\sum_{j=0}^n \frac{(-1)^j f(x_j)}{x-x_j}}{\sum_{j=0}^n \frac{(-1)^j}{x-x_j}} \quad (9)$$

which is a truly rational function. Berrut shows that this interpolant has no poles in  $R$ . The main purpose in this formula is that there is, in fact, a whole family of barycentric rational interpolants with arbitrarily high approximation orders which includes Berruts interpolant (9) as a special case. The construction is very simple. Choose any integer  $d$  with  $0 \leq d \leq n$ , and for each  $j = 0, 1, \dots, n-d$ , suppose  $q_j$  denotes the unique polynomial of degree at most  $d$  that interpolates  $f$  at  $d+1$

points  $x_j, x_{j+1}, \dots, x_{j+d}$ . Then let

$$P(x) = \frac{\sum_{j=0}^{n-d} \lambda_j(x) q_j(x)}{\sum_{j=0}^{n-d} \lambda_j(x)} \quad (10)$$

where

$$\lambda_j(x) = \frac{(-1)^j}{(x - x_j) \dots (x - x_{j+d})} \quad (11)$$

Thus,  $P$  is a blend of the polynomial interpolants  $q_0, q_1, \dots, q_{n-d}$ , with  $\lambda_0, \lambda_1, \dots, \lambda_{n-d}$  acting as the blending functions. Note that these functions  $\lambda_j$  only depend on the interpolation points  $x_j$ , so that the rational interpolant  $P$  depends linearly on the data  $f(x_i)$ . This construction gives a whole family of rational interpolants, one for each  $d = 0, 1, \dots, n$ , and it turns out that none of them have any poles in  $R$ .

In sum, the main properties of barycentric rational interpolation are as follows:

- 1-Polynomial interpolants can be evaluated fast and stably by the barycentric formula, even for thousands or more of interpolation points.
- 2-The barycentric formula has the form of a rational function, but reduces to a polynomial due to the use of specially-determined weights.
- 3-For all  $d, 0 \leq d \leq n$ , the rational function  $P(x)$  in (10) has no poles in  $R$ .
- 4-The rational form, for each evaluation of  $P(x)$  in point  $x$ , requires  $O(n)$  operations for each of the weights  $w_j$ , but the Lagrange form, requires  $O(n^2)$  additions and multiplications.

In the following sections, the main properties of the barycentric rational interpolation method for estimation of the required pixels for image zooming are elaborated.

### 3 Image zooming

In image zooming, a number of new pixels are placed among the original pixels of the image. The main aim is to estimate the quantity of the

unknown pixels. These pixels are determined on the basis of their neighboring pixels. There are two kinds of neighborhoods in images, namely 4-cell and 8-cell neighborhoods [32]. These neighborhoods are shown in Figure 1.

In most of the proposed methods, attempts are made to keep the zooming rate at a power of two, but it should be noted that this algorithm is applicable for every zooming rate.

Assume that dimensions of the original image,  $n \times n$ , spread regularly to  $(2n - 1) \times (2n - 1)$ . More precisely, if  $S(i, j)$  represents the pixel of the original image in the  $i^{th}$  row, and the  $j^{th}$  column, and  $Z(l, k)$  represent the pixel of the zoomed image in the  $l^{th}$  row and the  $k^{th}$  column, then the function  $f$ , defined by (12), places the values for the original image pixels in the interlaced places of the new image.

$$\begin{aligned} f : S &\rightarrow Z \\ f(S(i, j)) &= Z(2i - 1, 2j - 1) \\ i, j &= 1, 2, \dots, n \end{aligned} \quad (12)$$

The result can be seen in Figure 2. The original image pixels are shown with  $\bullet$  and the other pixels that must be estimated in several steps are shown with  $\circ$ .

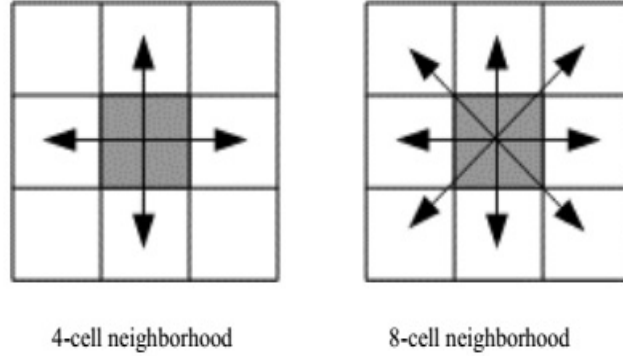


**Figure 1:** Types of neighborhoods

In this research, the first stage involved estimating the pixels with odd rows and even columns, the results of which is shown in Figure 3



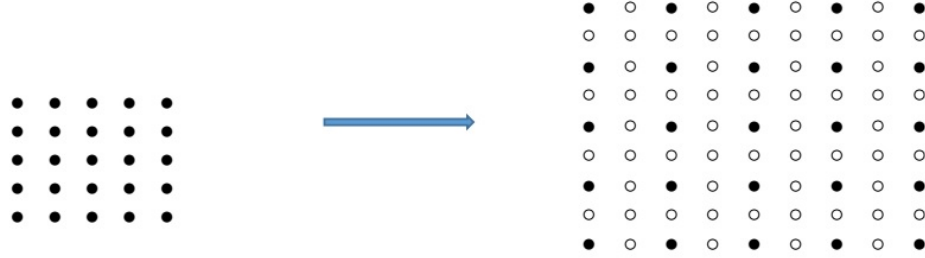


**Figure 2:** Image zooming

with the symbol "■".

The second stage, was to estimate the pixels with even rows and odd columns, the results of which is represented in Figure 4 with the symbol "◇".

In the third stage, the pixel estimation was performed with even rows and columns, the result of which is shown in Figure 5 and with the symbol □.

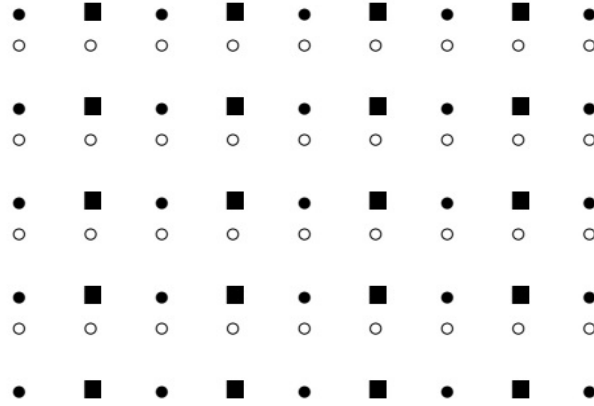


**Figure 3:** The first stage of pixels estimation.

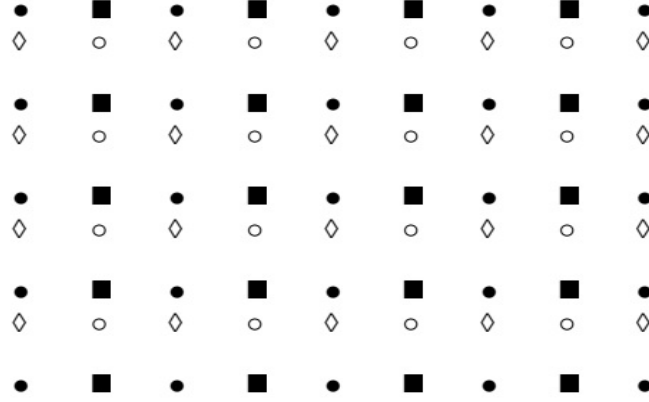


**Figure 4:** The second stage of pixels estimation.

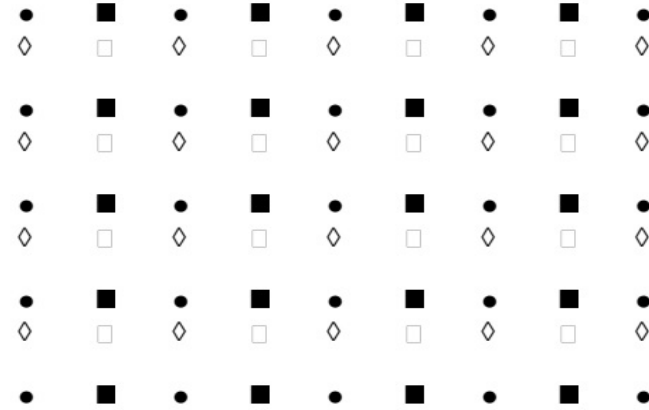


**Figure 5:** The third stage of pixels estimation.

## 4 The proposed method

In this method, the points are referred to as pixel coordinate of the image, whose brightness and number of columns and rows are considered as points in a 3D space. The required pixels were estimated using barycentric rational interpolation. Estimation of the required pixels were based on the 4-cell neighborhood or selection of the 4 original image pixels

in a row or a column. The intended point was selected, and then the intended pixels were estimated by selecting parameter  $d$  and calculating coefficients of barycentric rational interpolation.

The barycentric rational interpolation is used for real functions in a 1D space. Therefore, in order to be able to use this interpolation to estimate the value of pixels in an image, firstly we had to keep the row number constant. The four pixel values were chosen for distribution of the interpolation points, and then, after calculating their coefficients, three embedded pixels between them were estimated. This process was reiterated for subsequent pixels, with one overlapping pixel.

In case at the end, the number of pixels was less than four, the end pixel or the first one was repeated as needed. Similarly, by keeping the column number constant, the same process was repeated for the pixel estimation in the second stage. In order to estimate pixels in the third stage, we use average of 4-cell neighborhood. It should be noted that in order to approximate the pixels of the last column and row, pixels of the first and last of the average were used.

The steps in the procedure of the proposed method were as follows:

Step 1: Tuning the necessary parameters for the interpolation function, including the number of data and the  $d$  parameter.

Step 2: Implementation of the interpolation algorithm to estimate the number of unknown pixels in a line-by-line fashion.

Step 3: Implementation of the interpolation algorithm to estimate the number of unknown pixels in a column-by-column fashion.

Step 4: Estimating the remaining pixels using a quad point averaging method.

## 5 Experimental results

For the purpose of evaluation of the proposed method, a digital image was first considered as an original image for image zooming by factor of 2, and then it was reduced to half its size by removing its rows and columns alternately. Next, it was enlarged to double its size using the proposed method and the other existing methods. As expected, the more similar the original and the zoomed images were, the better was the performance of the algorithm.

The next section elaborates on the evaluation of quality metrics.

### 5.1 Assessment criteria

The PSNR and SSIM criteria were used to compare the two images in terms of their similarities. The greater the amount of PSNR and the closer the amount of SSIM was to one, the more was the conformity of the two images [33]. The measure PSNR was calculated based on (13) and (14):

$$\text{PSNR} = 10 * \text{Log}_{10}\left(\frac{\text{MAXI}^2}{\text{MSE}}\right) \quad (\text{dB}) \quad (13)$$

$$\text{MSE} = \frac{1}{mn} \sum_{i=0}^{m-1} \sum_{j=0}^{n-1} [I(i, j) - K(i, j)]^2 \quad (14)$$

where  $I(i, j)$  and  $K(i, j)$  are the pixels of the original image and the estimated image, respectively, and is the maximum amount of the image pixels.

The measure SSIM, which included the structural elements of the picture, measured the quality of the structural content and the similarity between the two images. This measure is a number between zero and one and is computed by (15). The closer the measure is to one, the more similar the two images are. However, the closer the measure is to zero, the less similar the two images are.

$$\text{SSIM}(x, y) = \frac{(2\mu_x\mu_y + c_1)(2\sigma_x\sigma_y + c_2)(\sigma_{xy} + c_3)}{(\mu_x^2 + \mu_y^2 + c_1)(\sigma_x^2 + \sigma_y^2 + c_2)(\sigma_x\sigma_y + c_3)} \quad (15)$$

where  $\mu$ ,  $\sigma^2$  and  $\sigma_{xy}$  are the mean, variance and co-variance of the pixels, respectively, and  $c_1$ ,  $c_2$  and  $c_3$  are three constants to prevent the fraction denominator from being zero.

### 5.2 Numerical experiments using the proposed method

The results of running the proposed algorithm in the MATLAB software are depicted in Table 1. In this Table, the measures PSNR and SSIM were used to zoom the image. Also 12 different standard images are shown in Figure 6, whose sizes are  $512 \times 512$  [34].



**Figure 6:** Different standard images for image zooming.

The results of the proposed method were analyzed and obtained using barycentric rational interpolation. In this method, the used values for  $d = 0, 1, 2$ , and the number points were considered to 4. For other proposed images, according to the PSNR value, the suitable value  $d$  will be equal to 1.

The findings are presented in Table 1. As one can see in this table, the average difference of PSNR between  $d = 1$  and  $d = 2$  is 0.13, and between  $d = 0$  and  $d = 1$  is 0.58. Also, the average difference of SSIM criterion for  $d = 1$  and  $d = 2$  is 0.0012, for  $d = 1$  and 0.0014 for  $d = 0$ . According to the obtained results, it can be concluded that a suitable value for parameter  $d$  for image zooming can be equal to 1.

To evaluate the proposed algorithm, analyses were done using barycen-

tric rational interpolation. Furthermore, this method was compared with Gaussian radial basis function (GRBF) [25], least square ellipsoid (LSE) methods [24], bi-linear interpolation (BIL) method, bi-cubic interpolation (BIC) method, and curvature interpolation method (CIM) [18].

The related results are illustrated in Table 2. As can be seen from the table, the average difference of PSNR between the proposed method and GRBF methods is 0.51, between proposed method and LSE is 0.80, and between the proposed method and CIM is 1.72. Also, the average difference of PSNR between the proposed method and BIC methods is 2.37 and between the proposed method and BIL method is 2.25.

based on the results of the comparative analysis it can be concluded that the proposed method has a better performance than the other methods on the selected image.

Figure 6 shows the sample image peppers zoomed with the proposed method and the other methods under study from a visual perspective. In addition, the differences between image zooming and original images are further shown in Figure 7. It can be observed that the images obtained from the proposed method are clearer and blur less with a good performance on the edges.

## 6 Conclusion

In this research, a new method of barycentric rational interpolation for image zooming has been presented. This method could significantly provide desirable results and preserve the image as well as the local structures around the edges.

Future studies can focus on developing the proposed method using modified edge correction techniques or non-linear methods, such as two-variable interpolation method. It would also be worthy to further investigate the effects of using intelligent algorithms on minimizing parameter  $d$  in future research projects.

**Table 1:** Results of running Barycentric rational interpolation with different d values using SSIM and PSNR, by factor of 2 in zooming.

Different	d=0		d=1		d=2	
Images	SSIM	PSNR	SSIM	PSNR	SSIM	PSNR
Lifting body	0.9737	36.03	0.9744	<b>36.43</b>	0.9724	35.96
Elaine	0.9526	34.14	0.9539	<b>34.46</b>	0.9514	34.12
Disk	0.9950	32.74	0.9954	<b>32.94</b>	0.9952	32.78
Peppers	0.9535	30.92	0.9549	<b>31.62</b>	0.9524	31.53
Fruits	0.9688	27.92	0.9715	<b>28.56</b>	0.9705	28.53
Dog	0.9802	33.49	0.9815	<b>34.01</b>	0.9806	33.97
Balloons	0.9876	31.87	0.9887	<b>31.89</b>	0.9883	31.53
Airplane	0.9808	31.62	0.9820	<b>32.47</b>	0.9803	32.15
Lena	0.9685	33.19	0.9699	<b>33.51</b>	0.9676	33.03
House	0.9850	33.43	0.9865	34.12	0.9861	<b>34.19</b>
Fire	0.9839	31.53	0.9855	32.51	0.9852	<b>32.76</b>
Swan	0.9818	32.44	0.9839	33.69	0.9836	<b>34.08</b>
Average	0.9759	32.44	0.9773	<b>33.02</b>	0.9761	32.89

**Table 2:** Comparison between Barycentric rational interpolation and the other methods by PSNR criterion by factor of 2 in zooming.

Methods	BIL	BIC	CIM	LSE	GRBF	Proposed method
Lifting body	33.34	33.30	33.87	35.28	35.92	<b>36.43</b>
Elaine	31.26	31.08	31.49	34.37	<b>34.58</b>	34.46
Disk	30.94	30.82	31.56	32.14	<b>33.00</b>	32.94
Fire	31.66	31.71	31.82	30.99	32.09	<b>32.76</b>
Swan	31.19	30.74	31.44	32.19	33.09	<b>34.08</b>
Dog	31.83	31.37	32.05	33.24	33.78	<b>34.01</b>
Balloons	31.29	31.73	32.28	33.18	<b>32.31</b>	31.89
House	32.64	32.60	32.97	33.54	33.83	<b>34.19</b>
Airplane	29.70	29.59	30.12	31.02	29.65	<b>32.47</b>
Lena	30.20	30.11	31.68	32.60	32.99	<b>33.51</b>
Fruits	27.17	27.08	27.49	27.82	28.41	<b>28.56</b>
Peppers	28.68	28.44	29.53	31.03	31.24	<b>31.62</b>
Average	30.83	30.71	31.36	32.28	32.57	<b>33.08</b>

**BIL****Difference between original image and  
BIL****LSE****Difference between original image and  
LSE****GRBF****Difference between original image and  
GRBF****Proposed method****Difference between original image and  
proposed method**

**Figure 7:** Results of Peppers image zooming by factor of 2 and using different methods.



## References

- [1] Lehmann, T., Gnner, C. Spitzer, K. (1999). Survey: Interpolation methods in medical image processing, *IEEE Trans. Med. Imaging.*, vol. 18, no. 11, pp. 1049-1075.
- [2] Lee, Y. J. Yoon, J. (2010). Nonlinear image upsampling method based on radial basis function interpolation, *IEEE Trans. Image Process.*, vol. 19, no. 10, pp. 2682-2692.
- [3] Keys, R. G. (1981). Cubic convolution interpolation for digital image processing, *IEEE Trans. Acoust., Speech, Signal Process.*, vol. 29, no. 6, pp. 1153-1160.
- [4] Hou, H. S. Andrews, H. C. (1978). Cubic splines for image interpolation and digital filtering, *IEEE Trans. Acoust., Speech, Signal Process.*, vol. 26, no. 6, pp. 508-517.
- [5] Thvenaz, P., Blu, T. Unser, M. (2000). Interpolation revisited, *IEEE Trans. Med. Image.*, vol. 19, no. 7, pp. 739-758.
- [6] Padmanabhan, S. A. Chandramathi, S. (2011). Image zooming using segmented polynomial interpolation in  $R^2$  space, *European Journal of Scientific Research*, vol. 57, no. 3, pp. 447-453.
- [7] Jensen, K. Anastassion, D. (1995). Subpixel edge localization and the interpolation of still images, *IEEE Trans. Image Process.*, vol. 4, no. 3, pp. 285-295.
- [8] Allebach, J. Wong, P. W. (1996). Edge-directed interpolation, in *Proc. IEEE Int. Conf. Image. Proc.*, vol. 3, pp. 707-710.
- [9] Carrato, S. Tenze, L. (2000). A high quality 2X image interpolator, *IEEE Signal Process.*, vol. 7, no. 6, pp. 132-135.
- [10] Li, X. Orchard, T. (2001). New edge directed interpolation, *IEEE Trans. Image Process.*, vol. 10, no. 10, pp. 1521-1527.
- [11] Cha, Y. Kim, S. (2007). The error-amended sharp edge (ease) scheme for image zooming, *IEEE Trans. Image Process.*, vol. 16, no. 6, pp. 1496-1505.

- [12] Li, M. Nguyen, T. Q. (2008). Markov random field model-based edge directed image interpolation, *IEEE Trans. Image Process.*, vol. 17, no. 7, pp. 1121-1128.
- [13] Zhang, X. Wu, X. (2008). Image interpolation by adaptive 2-D autoregressive modeling and soft-decision estimation, *IEEE Trans. Image Process.*, vol. 17, no. 6, pp. 887896.
- [14] Zhang, L. Wu, X. (2006). An edge-guided image interpolation algorithm via directional filtering and data fusion, *IEEE Trans. Image Process.*, vol. 15, no. 8, pp. 2226-2238.
- [15] Battiato, S., Gallo, G. stanco, F. (2002). A locally adaptive zooming algorithm for digital images, *Image and Vision Computing*, vol. 20, no. 11, pp. 805-812.
- [16] Jiang, H. Moloney, C. (2002). A new direction adaptive scheme for image interpolation, in *Proc. Int. Conf. Image Processing*, vol. 3, pp. 369-372.
- [17] Wang, Q. Ward, R. K. (2007). A new orientation-adaptive interpolation method, *IEEE Trans. Image Process.*, vol. 16, no. 4, pp. 889990.
- [18] Kim, H., Cha, Y. Kim, S. (2011). Curvature interpolation method for image zooming, *IEEE Trans. Image Process.*, vol. 20, no. 7, pp. 1895-1903.
- [19] Nowrozian, N. Hassanpour, H. (2014). Image zooming using non-linear partial differential equation, *International Journal of Engineering Transactions A: Basics*, vol. 27, no. 1, pp. 15-28.
- [20] Warbhe, S. Gomes, J. (2016). Interpolation technique using non-linear partial differential equation with edge directed bi-cubic, *International Journal of Image Processing*, vol. 10, no. 4, pp. 205-213.
- [21] Lee, Y. J. Yoon, J. (2010). Nonlinear image upsampling method based on radial basis function, *IEEE Trans. Image Process.*, vol. 19, no. 10, pp. 26822692.

- [22] Youssef, D., Mohammed, B., Abdelmalek, A., Tarik, H. EL Miloud, J. (2015). Zoom and restoring of digital image artificial neural networks, *Computer Science and Engineering*, vol. 5, no. 1, pp. 14-24.
- [23] Lee, Y.J. Yoon, J. (2015). Image zooming method using edge-directed moving least squares interpolation based on exponential polynomials, *Applied Mathematics and Computation*, vol. 269, pp. 569-583.
- [24] Esmaili Zaini, A. M., Barid Loghmani, G. Latif, A. M. (2016). Image magnification by least squares surfaces, *Iranian Journal of Numerical Analysis and Optimization*. In press.
- [25] Esmaili Zaini, A. M., Latif, A. M. Barid Loghmani, G. (2017). Tuning shape parameter of radial basis functions in zooming images using genetic algorithm, *Journal of AI and Data Mining*. In press.
- [26] Stoer, J., Bulirsch, R. (2013). *Introduction to numerical analysis* (Vol. 12). Springer Science Business Media.
- [27] Berrut, J. P., Trefethen, L. N. (2004). Barycentric lagrange interpolation. *Siam Review*, 46(3), 501-517.
- [28] Rutishauser, H. (2012). *Lectures on numerical mathematics*. Springer Science Business Media.
- [29] Berrut, J. P., Baltensperger, R., Mittelmann, H. D. (2005). Recent developments in barycentric rational interpolation. *Trends and applications in constructive approximation*, 151, 27-51.[30]
- [30] Trefethen, L. N. (2013). *Approximation theory and approximation practice*. Siam.
- [31] Floater, M. S., Hormann, K. (2007). Barycentric rational interpolation with no poles and high rates of approximation. *Numerische Mathematik*, 107(2), 315-331.
- [32] Gonzalez, R. C., Woods, R. E. (2002). *Digital image processing* prentice hall. Upper Saddle River, NJ.

- [33] Wang, Z., et al. (2004). Image quality assessment: from error visibility to structural similarity, IEEE Trans. Image Process., vol. 13, no. 4, pp. 600-612.
- [34] Online. Available: [www.freeimages.co.uk](http://www.freeimages.co.uk) and [sipi.usc.edu](http://sipi.usc.edu).

**Ali Mohammad Esmaili Zaini**

Department of Applied Mathematics  
PhD candidate in Applied Mathematics  
Yazd University  
Yazd, Iran  
E-mail: [esmailizaini@stu.yazd.ac.ir](mailto:esmailizaini@stu.yazd.ac.ir)

**Ghasem Barid Loghmani**

Department of Applied Mathematics  
Professor of Mathematics  
Yazd University  
Yazd, Iran  
E-mail: [loghmani@yazd.ac.ir](mailto:loghmani@yazd.ac.ir)

**Ali Mohammad Latif**

Department of Computer Engineering  
Associate Professor  
Yazd University  
Yazd, Iran  
E-mail: [alatif@yazd.ac.ir](mailto:alatif@yazd.ac.ir)